Bulletin of the JSME Vol.11, No.2, 2024
Mechanical Engineering Journal

# Multi-fluid simulation of pool scrubbing in the bubble rise region of PECA experiment

Matic KUNŠEK*,**, Leon CIZELJ*,** and Ivo KLJENAK*,**
*Jozef Stefan Institute
Jamova cesta 39, Ljubljana SI-1000, Slovenia
**University of Ljubljana, Faculty of Mathematics and Physics
Jadranska ulica 19, Ljubljana SI-1000, Slovenia
E-mail: ivo.kljenak@ijs.si

**Received: 25 October 2023; Revised: 29 November 2023; Accepted: 10 January 2024**

**Abstract**
Theoretical simulations of dispersed solid particle behaviour inside a scrubbing pool within the bubble rise region are presented. The goal is to evaluate the decontamination factor of the particles during the pool scrubbing process. The basic phenomena of pool scrubbing are described. The setup used for the simulation validation is presented. Then, the boundary and initial conditions of the PECA experiments, which were performed at CIEMAT (Madrid, Spain) and were used for simulations, are presented. The subgrid model for decontamination through transfer of particles from gas bubbles to the surrounding liquid is described. The calculation results are evaluated and compared with the part of the PECA experimental results to which the proposed modelling is applicable.

***Keywords*** : Aerosols, Pool scrubbing, PECA experiment, Multi-fluid simulation

## 1. Introduction

During a hypothetical severe accident in a light water reactor nuclear power plant, the fuel could melt and there is a possibility, that some of the radioactive material could be released as particles to the surrounding area. The releases of the radioactive material can be reduced with the application of pool scrubbing, where contaminated gases are filtered through a pool of liquid water. To understand what happens during pool scrubbing, phenomena at the local scale need to be understood. Specifically, since the gases enter the scrubbing pool as a jet that disperses into bubbles, studying the behaviour of the particle removal from the bubbles is crucial to understand pool scrubbing phenomena.

Pool scrubbing has been investigated experimentally as well as theoretically. Among experiments, some of those relevant for the present work, that is in which bubble plumes occurred, have been described by Turni (2016), Kuhlman et al. (1986) and Uchida et al. (2016). The first two experiments have already been simulated in the authors' earlier work (Kunšek et al., 2022). Due to the complexity of pool scrubbing phenomena on one side, and the necessity to predict gas decontamination in safety analyses on the other side, empirical models were developed and included in several computer codes in the last decades of the past century (Berna et al., 2016): SUPRA (Wassel et al., 1985), BUSCA (Ramsdale et al., 1991) and SPARC (Owczarski and Burk, 1991). Some latest developments of empirical models have been proposed by Uchida et al. (2016), partially based on earlier work by Kaneko et al. (1992). As to theoretical studies, to the best of the authors' knowledge, the authors' earlier work (Kunšek et al., 2022), from which the method was applied in the present work, was the first attempt to simulate pool scrubbing experiments with a multi-fluid description, which is based on first physical principles.

In the present paper, the pool scrubbing PECA experiment (Peyres et al., 1995), performed at CIEMAT (Centro de Investigaciones Energéticas, Medioambientales y Tecnológicas) in Madrid (Spain) was simulated using multi-fluid modelling. The simulation was performed using the open-source Computational Fluid Dynamics (CFD) code OpenFoam (Greenshields, 2015). The proposed approach considers only the decontamination in the rise region of pool scrubbing,

Paper No.23-00488
J-STAGE Advance Publication date : 24 January, 2024
[DOI: 10.1299/mej.23-00488]

hence it is applicable only to a part of PECA experimental results. In the modelling, four different fluids are considered: gas, liquid and two particle fluids (particle fluid 1 within gas bubbles and particle fluid 2 within liquid). All fluids are described in the Eulerian frame. The particles transport from bubbles to liquid during the bubble rise in the scrubbing pool is simulated as a transfer via a subgrid model from particle fluid 1 to particle fluid 2, based on previous simulations of particle motion within bubbles. Namely, the subgrid model takes into account that, due to bubbles rising, the inner gas motion moves particles inside bubbles (particle fluid 1) due to interfacial drag. The particles first migrate towards the bubble surface and then out into the liquid (to become part of particle fluid 2). The particle densities and bubble diameters were prescribed, based on data from the literature. The simulation results were analysed and the decontamination factor, which is the resulting measure of the scrubbing efficiency, was calculated and compared with the experimental measurement.

## 2. Basic phenomenology and quantitative description of pool scrubbing

The goal of pool scrubbing is to remove as much radioactive substances as possible (which can be gases or particles) from a mixture of condensable and non-condensable gases that pass through the liquid pool (in most cases filled with water). An additional purpose is to condense steam and, with this, reduce a possible pressure surge in the nuclear power plant containment. Because of the different behaviour of mixture and scales of interactions, three regions can be defined (OECD/NEA, 1999; Herranz and Fontanet, 2013): injector region around the inlet, rise region and surface region. The injector region is usually characterised by an intense mixing, due to the injection of a gas jet into a quiescent liquid. Although a significant transport of particles from the gas to the liquid occurs in this region, the modelling of particle transfer from the gas to the liquid phase that would consider basic phenomena is beyond the possibilities of present-day numerical simulations, as the time and length scales are comparable to those of turbulent flow. In the rise region, the gas flows through the liquid in the form of bubbles, and the basic mechanisms of particle transport from within the bubbles to the gas-liquid interphase and further into the liquid phase may at least be inferred, if not mathematically described in detail. In the surface region, bubbles burst, releasing the remaining particles into the atmosphere above the pool. The accurate estimation of the mass of these particles depends on the accuracy of the modelling of the filtration in the previous two regions.

The main quantitative parameter that describes the successfulness of the particle removal in pool scrubbing is the scrubbing or filtration efficiency ($\beta$). This efficiency is usually expressed in terms of the Decontamination Factor ($DF$), which is defined as the ratio of the radioactive material mass entering and leaving the pool with the gaseous phase:

$$DF = \frac{m_{in}}{m_{out}} = \frac{1}{1-\beta}, \tag{1}$$

where $m_{in}$ represents the mass entering the pool and $m_{out}$ the mass leaving the pool. The $DF$ is also highly affected by the pool temperature, which is especially true for installations with higher steam fraction in the mixture entering the pool (Uchida et al., 2016). When the pool scrubbing region may be divided in different parts, characterized by different phenomena (as stated before), the overall $DF$ can be calculated as a product of $DF$ for each separate region.

## 3. PECA experiment

PECA is an experimental facility at CIEMAT (Peyres et al., 1995; Herranz et al., 1997). The goal of the experimental facility is to determine the decontamination factor of pool scrubbing and to enable the verification of various system codes used for simulation of severe accident phenomena (MAAP, STCP, MELCOR, BUSCA, SPARC). The layout of the facility is shown in Figure 1. The facility is cylindrically shaped with height of 4.35 m and radius of 0.75 m. The top and bottom heads are rounded with height of 0.338 m. The full central line height is 5.03 m.

The structure is built from stainless steel and was designed to sustain pressures up to $3.5 \cdot 10^5$ Pa and temperatures up to 140 °C. It has a series of windows placed at different elevations and angles for visual tracking of phenomena in the pool. The aerosol generation system is a solid particle dispenser and produces particles in diameter range from 0.5 μm up to 100 μm with mass flow rates from 40 mg/h up to 25 g/h for particle density of 1 g/cm$^3$.

The aerosols are particles of nickel (Ni), which has a density of 8908 kg/m$^3$, with AMMD (Aerosol Mass Median

[DOI: 10.1299/mej.23-00488]

Diameter) of 3 μm. The aerosols samples are taken from three different locations: the injection line, the pool and the vessel atmosphere above the pool. In all considered experimental cases, the gas volumetric flow at the inlet was 0.003 $m^3/s$ and the particle mass flow rate was 0.6 mg/s. The decontamination factors were measured at different elevations in the pool and at elevations above the pool surface. The measured decontamination factors of the considered experiments (referred as RCA1, RCA2, RCA3 and RCA4, where RCA is the abbreviation of "Reinforced Concerted Action"), at elevation 0.5 m above the pool surface (which are relevant for this study), are shown in Table 1.

The experiments were performed with different submergences (vertical distance between gas injection and pool surface). As the elevation of gas injection was fixed, the elevation of the pool surface was varied. In all experimental cases, the injection region, as described above, was present above the gas inlet. Since the model proposed in the present work is suitable only for the bubble rise region, the modelling considered the experimental case RCA4 between elevations 1.25 m and 2.5 m. At this location we can, quite confidently, assume that the region is (most probably) the rise region. To compare the experimental results with the theoretical ones, the experimental decontamination of the first 1.25 m was taken from the results of the experimental case RCA3. Of course, the decontamination in the first 1.25 m for cases RCA3 and RCA4 differ due to the different hydrostatic pressure; however, in the present work, it was assumed that this difference is not significant. Therefore, the theoretical model considers the case RCA4 from elevation 1.25 m to 2.5 m and takes the initial conditions from the results of experimental case RCA3 (elevation 1.25 m). This means that decontamination was simulated over a height of 1.25 m.

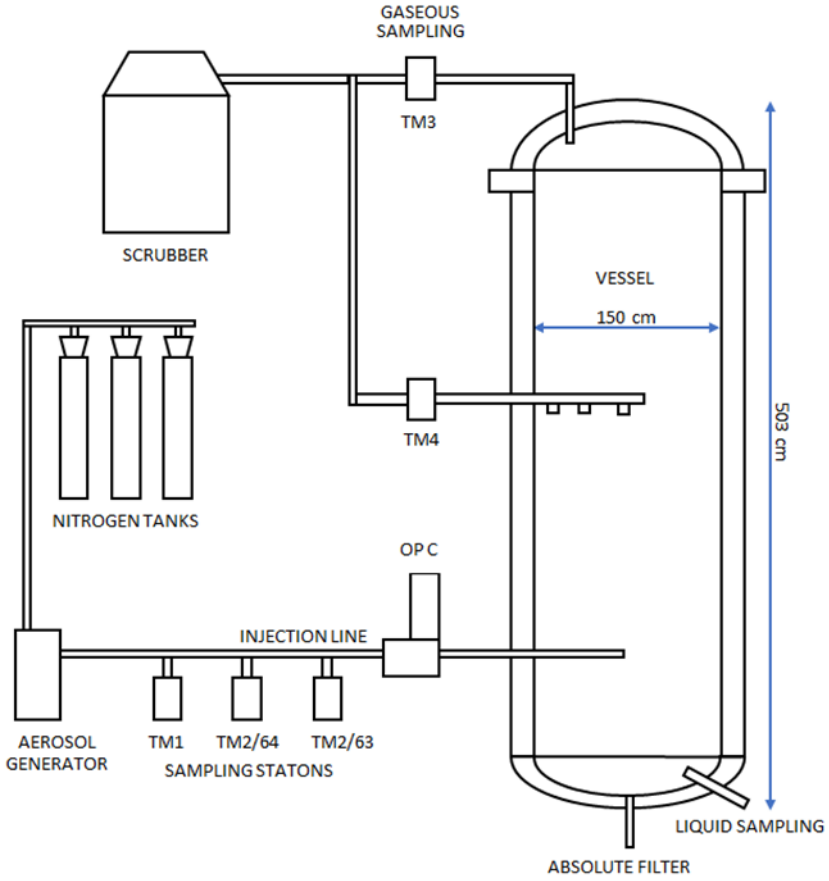


Fig. 1 Layout of PECA facility (inspired by Herranz et al., 1997).
TM: sample points; OPC: Optical Particle Counter.

[DOI: 10.1299/mej.23-00488]

Table 1 PECA experimental results.

| Case | Submergence (m) | $DF_{min}$ | $DF_{mean}$ | $DF_{max}$ |
|---|---|---|---|---|
| RCA1 | 0.25 | 12.4 | 12.8 | 13.2 |
| RCA2 | 0.50 | 16 | 28.25 | 40.5 |
| RCA3 | 1.25 | 46.6 | 63.3 | 80 |
| RCA4 | 2.50 | 719 | 969.85 | 1220.7 |

## 4. Theoretical modelling

The importance of the theoretical modelling, using numerical simulations, for the investigation of pool scrubbing is increasing and contributes to experimental investigations, which are costly and time consuming. However, computers are still not powerful enough to directly solve the Navier-Stokes equations for multi-phase flows in large domains (Rusche, 2003; Ničeno et al., 2009).

One of the better-suited approaches for relatively large systems, to be modelled using a much lower number of numerical cells than if the phases were considered separately, is two-fluid (or multi-fluid) modelling (OECD/NEA, 1999; Frank et al., 2004). All phases are treated as inter-penetrating continua, represented by averaged conservation equations. The averaging process adds the phase fraction for each phase into the equation set, which is defined as the probability that this phase is present at the observed location.

The inter-phase momentum transfer is phase-fraction dependent and is determined from the instantaneous forces acting on the dispersed phase, comprising drag, lift and virtual mass. Problems arise from complex interactions between the fluids, which have different interactions depending on the volume fraction of each fluid at the observed location. In order to obtain a numerical solution, the calculation domain has to be divided into calculation cells. Because a higher number of cells directly corresponds to a longer computation time, models for subgrid scales are used in most multi-fluid simulations. Because these models do not need large numbers of cells to run, they are well-suited for use in industrial and nuclear installations. The current state of modelling techniques is described by Bonart (2012). In short, the particle transport is modelled with the use of transport equations, which may take into account size distribution, coagulation, deposition and mechanical resuspension of particles.

In the present work, the same theoretical model was used as in the authors' previous work (Kunšek et al., 2022). The simulation of single bubble scrubbing was performed using the transient multi-phase solver reacting-MultiphaseEulerFoam, which is part of the open-source CFD software OpenFoam 3.0.0 and is based on the finite volume method of equation discretization. In the simulation, a multi-dimensional case for four incompressible phases (liquid, gas, particles 1 and particles 2) was calculated. The only mass transfer occurs via the subgrid model for phase pair particles 1 and particles 2, which is explained in detail by Kunšek et al. (2022). This model was determined by first simulating (using a two-fluid modelling approach) the flow of particles within bubbles, entrained by the gas motion induced by the bubble rise through the liquid. The results of the deposition rate of particles on the bubble surface were fitted as a function that describes the decrease of the particle volume fraction within bubbles, which was then implemented into the four-field fluid model:

$$\frac{\partial \alpha_{particle}}{\partial t} = D \cdot \omega \cdot {d_{bubble}}^3 \cdot \alpha_{particle} \cdot \left(1 + \frac{C}{D} \cdot {\alpha_{particle}}^2\right), \tag{2}$$

where $d_{bubble}$ is the bubble diameter, $C$ and $D$ are constants, determined so that the function fits the simulation results of particle deposition on the bubble surface, and the bubble interface rotational velocity $\omega$ results from the relative velocity between the gas and liquid phases:

$$\omega = \frac{|\vec{v_r}|}{r_{bubble}} = \frac{2\left|\vec{v}_g - \vec{v}_l\right|}{d_{bubble}}, \tag{3}$$

where $\vec{v}_r$ is the relative velocity between the phases, $r_{bubble}$ is the bubble radius, $\vec{v}_g$ is the gas velocity and $\vec{v}_l$ is the liquid velocity. This function thus determined the transfer rate from particles 1 to particles 2. There was no mass transfer

[DOI: 10.1299/mej.23-00488]

between other phase pairs. The multi-phase solver uses standard multi-phase balance equations for mass, momentum and energy for each phase, which are solved by the PIMPLE coupling algorithm (Greenshields, 2015). The following equations are being solved:

— mass conservation equation:

$$\frac{\partial \alpha_i \rho_i}{\partial t} + \nabla(\alpha_i \rho_i \vec{v}_i) = \Gamma_i \,, \tag{4}$$

where $\alpha_i$ is the volume fraction of phase $i$, $\rho_i$ the phase $i$ density, $\vec{v}_i$ the phase $i$ velocity and $\Gamma_i$ the inter-phase mass transfer rate of phase $i$.

— momentum balance equation:

$$\frac{\partial \alpha_i \rho_i \overrightarrow{v_i}}{\partial t} = -\vec{\nabla}(\alpha_i \rho_i \vec{v}_i \vec{v}_i) - \alpha_i \vec{\nabla} p_i + \vec{\nabla}\alpha_i(\bar{\bar{\tau}}_i + \tau_i^t) + \alpha_i \rho_i \vec{g} + \vec{v}_i \Gamma_i + \overrightarrow{M_\iota} \,, \tag{5}$$

where $\vec{\nabla} p_i$ is the pressure gadient of phase $i$, $\bar{\bar{\tau}}_i$ the average viscous stress of phase $i$, $\tau_i^t$ the Reynolds stress of phase $i$, $\vec{g}$ the gravity and $\overrightarrow{M_\iota}$ the average inter-phase momentum transfer rate of phase $i$. The virtual mass force on bubbles was calculated from:

$$\overrightarrow{F_{vm}} = C_{vm} \rho_g V \left( \frac{D\overrightarrow{v_g}}{Dt} - \frac{D\overrightarrow{v_\iota}}{Dt} \right), \tag{6}$$

where $C_{vm}$ is the virtual mass force coefficient, $\rho_g$ the gas density, $V$ the bubble or particle volume, $\overrightarrow{v_g}$ the bubble velocity and $\overrightarrow{v_l}$ the liquid velocity. The lift force on bubbles was calculated from:

$$\overrightarrow{F_l} = C_l \rho_g V \overrightarrow{v_r} \times (\nabla \times \overrightarrow{v_\iota}), \tag{7}$$

where $C_l$ is the lift force coefficient, $\rho_g$ the gas density, $V$ the bubble or particle volume, $\overrightarrow{v_r}$ the bubble relative velocity and $\overrightarrow{v_l}$ the liquid velocity. These forces, as well as the drag force $\overrightarrow{F_d}$, are included in the momentum equation through the interface momentum transfer term $\overrightarrow{M_\iota}$:

$$\overrightarrow{M_\iota} = \left(\overrightarrow{F_d} + \overrightarrow{F_l} + \overrightarrow{F_{vm}}\right) \frac{\alpha_g}{V_p}, \tag{8}$$

where $\alpha_g$ is the volume fraction of the dispersed phase and $V_p$ the volume of particle or bubble.

— energy conservation equation:

$$\frac{\partial \alpha_i \rho_i H_i}{\partial t} = -\vec{\nabla}(\alpha_i \rho_i H_i \vec{v}_i) - \vec{\nabla}\alpha_i(\bar{\bar{q}}_i + q_i^t) + \alpha_i \frac{Dp_i}{Dt} + H_i \Gamma_i + q_{ki}'' a_i + \Phi_i \tag{9}$$

where $H_i$ is the specific enthalpy of phase $i$, $\bar{\bar{q}}_i$ the conductive heat flux, $q_i^t$ the turbulence enhanced heat flux, $Dp_i/Dt$ the reversible rate of enthalpy change due to compression, $q_{ki}''$ the conductive heat flux between phases, $a_i$ the interfacial area concentration and $\Phi_\mathrm{i}$ the heat source for phase $i$. The interfacial area density $a_\mathrm{i}$ was calculated from the following equation (Ozaki et al., 2018):

$$a_\mathrm{i} = \frac{6 \cdot \alpha_g}{d_p}, \tag{10}$$

[DOI: 10.1299/mej.23-00488]

where $\alpha_g$ is the volume fraction of the dispersed phase and $d_p$ the particle or bubble diameter.

In the simulation, for air in water, the lift and virtual mass coefficients were set to 0.5 and the turbulent dispersion coefficient was set to 0.05. The used drag model was the Schiller-Naumann model (Wardle and Weller, 2013):

$$\overrightarrow{M_i} = \sum_j \frac{3}{4}\rho_j \alpha_i \alpha_j C_D \frac{\left|\overrightarrow{v_i} - \overrightarrow{v_j}\right|\left(\overrightarrow{v_i} - \overrightarrow{v_j}\right)}{d_i}, \tag{11}$$

$$C_D = \begin{cases} \dfrac{24(1 + 0.15Re^{0.683})}{Re}, & Re \leq 1000 \\ 0.44, & Re > 1000 \end{cases} \tag{12}$$

where $C_D$ is the drag coefficient, $d_i$ the dispersed phase diameter and $Re$ the Reynolds number.

The drag between the undesired phase pairs (gas-particles 2, liquid-particles 1 and particles 1-particles 2) was multiplied by $10^{-3}$ to simulate that the particle phase 1 is connected with the gas phase and the particle phase 2 with the liquid phase. Namely, in a multi-phase model, phases act on each other via drag. By multiplication by a small number, the drag between an undesired phase pair becomes negligible and the equations become "semi-separated". The four momentum equations in the solver can therefore become separated to gas-particles 1 part and liquid-particles 2 part. This corresponds to the idea of the subgrid model, where particle phase 1 does not interact with liquid and particle phase 2 does not interact with gas. The multiplication factor ($10^{-3}$) was chosen arbitrarily. The model also considers only the decontamination of dispersed spherical bubbles with no interaction between them.

Both particle phases were simulated as a dispersed liquid phase with a droplet diameter of 3 μm which corresponds to the AMMD of particles in the PECA experiment (Herranz et al., 1997). Namely, the difference in dispersed solid or dispersed liquid phase in the OpenFoam solver is only in the phase density change according to local parameters (Greenshields, 2015), which is, for this case, negligible.

Despite the assumptions in the modelling, sometimes reducing complex phenomena to very simple ones, as well as the multi-fluid approach that considers the gas, liquid and particles as an inhomogeneous mixture, the proposed model is one of the first attempts to describe pool scrubbing (at least in the bubble rise region) using physically-based quantities.

## 5. Computational domain, mesh, boundary and initial conditions

A numerical mesh representing a cylinder with radius of 0.75 m and height of 1.75 m was developed. Since the particle removal model (Kunšek et al., 2015) is suitable only for the rise region of pool scrubbing, the numerical simulation was also performed only for that part (as already explained earlier). The inlet area was therefore large and the inlet radius of 5 cm was based on the bubble plume radius on the pictures taken at the experimental facility (Peyres et al., 1995; Herranz et al., 1997).

The numerical mesh was developed using the OpenFoam utility snappyHexMesh and is composed of around 209,000 computational cells. The suitability of the mesh size was verified in earlier work (Kunšek et al., 2022).

The boundary conditions of the cases on the inlet were air and particle velocity of 0.363 m/s and particle volume fraction of $2.25 \cdot 10^{-8}$; the remaining volume fraction was air as were the conditions in PECA experiment, which are the conditions at the pool surface of the experimental case RCA3. The outlet was specified as an opening with constant pressure $10^5$ Pa and free outlet condition for volume fraction with air fraction 1 for returning flow. The walls were treated with no-slip condition for velocity fields and as zero gradient for phase fractions.

The initial conditions were water up to 1.25 m (the pool depth difference between the experimental cases RCA4 and RCA3, which had depths of 2.5 m and 1.25 m, respectively), topped with 0.5 m of air. The liquid phase also included the initial seeding for every other phase (particle phases and gas phase with volume fraction $10^{-12}$) to prevent discontinuities. The initial velocity field was set to 0 m/s.

## 6. Results and discussion

To compare the simulation results with the PECA experiment, the average decontamination factor was calculated as

[DOI: 10.1299/mej.23-00488]

the ratio of the sums of particles 1 mass fluxes entering ($\dot{m}_{p\_in}(t)$) and exiting ($\dot{m}_{p\_out}(t)$) the computational domain in $10^{-2}$ s time intervals:

$$DF = \frac{\sum \dot{m}_{p_{in}}(t)}{\sum \dot{m}_{p_{out}}(t)}. \tag{13}$$

The first few seconds of the simulation were scrapped because the bubbles need some time to reach the upper domain boundary. The approximate cut-off time was set by the arrival of air to the water surface (5 s). In this way, a decontamination factor of 17.52 was calculated.

Since in the simulation only the rise region is considered, and the experimental results consider the whole tank, the decontamination factor is compared with the quotient of the experimental decontamination factors from runs RCA4 and RCA3. This gives us the mean experimental decontamination factor of 15.32 with 30 % error bounds.

The comparison of the experimental and theoretical results shows a very good agreement (Figure 2, where error bounds are also indicated). However, since the radius of the inlet in the numerical simulation is set to 5 cm based on the measurement from the picture of bubble plume from the experiment, a study of variation of the inlet radius was performed. Namely, as the simulation starts at level 1.25 m, this "inlet" is fictional, and the radius indicates the dimension of the horizontal cross-section on which the gas phase is dispersed. The inlet radii were prescribed in 1 cm steps from inlet radius 2 cm up to inlet radius 10 cm. The inlet volumetric flow rate was kept constant for all cases. Thus, a wider inlet causes a lower local gas volume fraction, and vice-versa. The results are shown in Fig. 2. The decontamination factor decreased with increasing inlet radius because, at the conditions of the simulated experiment, the effect of slower gas circulation within bubbles due to lower initial gas velocity (at the begining of the bubble rise region, where the influence of the jet region might still be present) prevailed over the longer times the bubbles stay in the liquid, due to lower initial gas velocity as well. The large majority of inlet sizes give satisfactory results, with the inlet with radius in the range between 6 cm and 8 cm giving the best ones. This indicates that in the experiment, bubbles might have been spread over a region of such dimensions. Of course, it cannot be excluded that the prescribed inlet radius compensates some model deficiencies. However, at present, this cannot be verified due to the lack of additional tests in the same experimental facility (so that the number of tests would be higher than the number of degrees of freedom in the modelling).

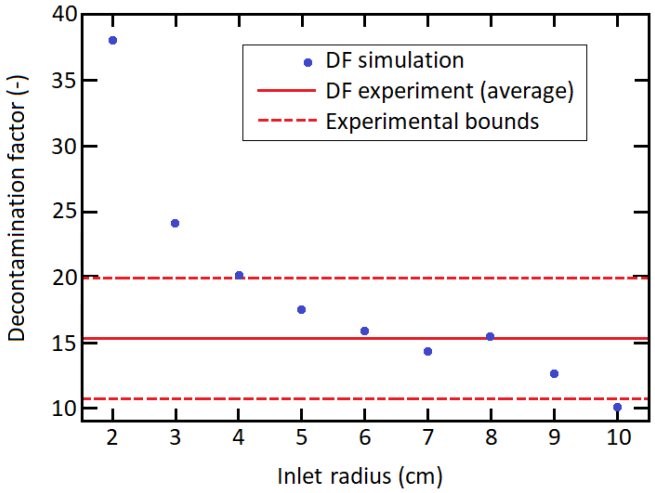


Fig. 2 Calculated decontamination factor depending on inlet radius.

In the experiment, the bubble sizes were measured in detail around the inlet area. However, no measurements were performed in the upper part of the experimental facility which is interesting for our study. Therefore, simulations to determine the effect of the bubble diameter variation on the calculated decontamination factor were performed. The bubble diameters tested were 0.25, 0.35, 0.5, 0.7, 1, 1.3, 1.7 and 2.2 cm. The results are shown on Fig. 3. The

[DOI: 10.1299/mej.23-00488]

decontamination rate increased with increasing bubble diameter because, at the conditions of the simulated experiment, the effect of faster gas circulation within the bubble due to higher gas velocity of larger bubbles (in the simulated range of bubble sizes) prevailed over the slower particle deposition due to larger bubble size as well. The simulations performed with bubble diameters 0.25 and 0.35 cm give the best results. The results for bubbles with diameters equal or greater than 1.7 cm give the worst results, since bubbles of that size are usually not observed in dispersed bubble flow in pools.

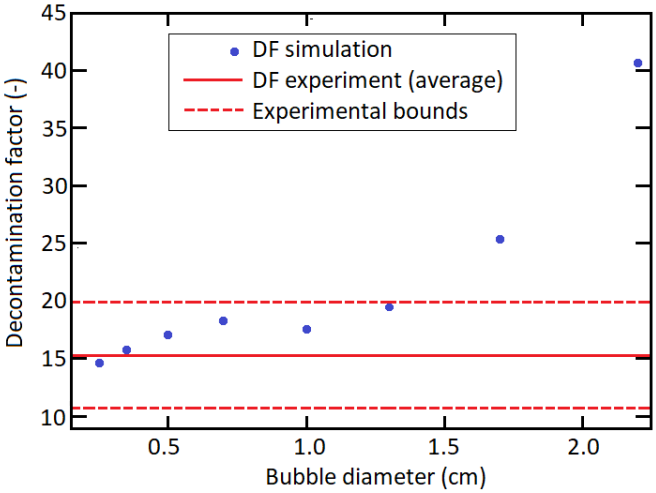


Fig. 3 Calculated decontamination factor depending on bubble diameter.

One of the important causes for the observed differences could be that the average calculated particle volume fraction is around $10^{-8}$, which could lead to numerical errors. Also, the proposed model does not include the particle removal in the gaseous phase at the top of the scrubbing tank.

## 7. Conclusions

A simulation of the PECA decontamination experiment of an air-particle mixture in a pool scrubbing tank with a proposed subgrid model using a CFD solver with multi-phase modelling approach was performed. The Euler-Euler description was used with the goal of studying large quantities of particles in large pools. However, the use of such description means operating with extremely low volume fractions of the particle phase which could lead to numerical errors. Nevertheless, the subgrid model gives good results in comparison with the experimental results from the PECA facility.

Further developments of the modelling could consist in adding different flow regimes, cap bubble decontamination and also bubble breakage, coalescence and collisions to the subgrid modelling. Other pool scrubbing regions (jet inlet and surface region) should also be added to the studies to be able to quantitatively compare simulations with entire experiments.

## Acknowledgements

The authors acknowledge the financial support from the Slovenian Research Agency through grant P2-0026.

## References

Berna, C., Escrivá, A., Muñoz-Cobo, J.L. and Herranz, L.E., Enhancement of the SPARC90 code to pool scrubbing events under jet injection regime, Nuclear Engineering and Design, Vol. 300 (2016), pp. 563-577.

Bonart, H., Implementation and validation of a solver for direct numerical simulations of turbulent reacting flows in OpenFoam (2012), Bachelor Thesis, Karlsruhe Institute of Technology, Germany.

Frank, T., Shi, J. and Burns, A.D., Validation of Eulerian multiphase flow models for nuclear safety application, 3rd International Symposium on Two-Phase Flow Modelling and Experimentation (2004), Pisa, Italy.

[DOI: 10.1299/mej.23-00488]

Greenshields, C., OpenFoam User Guide, OpenFOAM Foundation Ltd (2015), version 3.

Herranz, L.E., Peyrés, V., Polo, J., Escudero, M.J., Espigares, M.M. and López-Jiménez, J., Experimental and analytical study on pool scrubbing under jet injection regime, Nuclear Technology, Vol. 120 (1997), pp. 95-109.

Herranz, L. and Fontanet, J., Analysis of the effect of water ponds on HTR confinement behavior under accident conditions, Progress in Nuclear Energy, Vol. 67 (2013), pp. 7-14.

Kaneko, I., Fukasawa, M., Naitoh, M., Miyata, K. and Matsumoto, M., Experimental study on aerosol removal effects by pool scrubbing, Proceedings of the 22nd DOE/NRI Nuclear Air Cleaning Conference, 24-27 August 1992, Denver, USA (as cited by Uchida et al., 2016).

Kuhlman, M.R., Gieseke, J.A., Merilo, M. and Oehlberg, R., Scrubbing of fission product aerosols in LWR water pools under severe accident conditions (1986), Proceedings of the Symposium on Source Term Evaluation for Accident Conditions, Columbus, OH, USA, 28 October - 1 November 1985.

Kunšek, M., Cizelj, L. and Kljenak, I., New multi-fluid model of pool scrubbing in bubble rise region, Nuclear Engineering and Design, Vol. 395 (2022), p. 111873.

Ničeno, B., Boucker, M. and Smith, B., Euler-Euler large eddy simulation of a square cross-sectional bubble column using the Neptune_CFD code, Science and Technology of Nuclear Installations (2009), pp. 1-8.

OECD/NEA, OECD/CSNI Specialist Meeting on Nuclear Aerosols in Reactor Safety-Summary and Conclusions, OECD Nuclear Energy Agency/CSNI, NEA/CSNI/R(99)5 (1999), Cologne, Germany.

Owczarski, P.C. and Burk, K.W., SPARC-90: A code for calculating fission product capture in suppression pools, NUREG/CR-5765 (1991), U.S. Nuclear Regulatory Commission (as cited by Berna et al., 2016).

Ozaki, T., Hibiki, T., Miwa, S. and Mori, M., Code performance with improved two-group interfacial area concentration correlation for one-dimensional forced convective two-phase flow simulation, Journal of Nuclear Science and Technology (2018), pp. 1-20.

Peyres, V., Espigares, M.M., Polo, J., Escudero, M.J., Herranz, L.E. and López-Jiménez, J., Pool scrubbing and hydrodynamic experiments on jet injection regime, Report 785 (1995), Centro de Investigaciones Energeticas, Madrid, Spain.

Ramsdale, S., Friederichs, H.-G., and Güntay, S., BUSCA JUN91: Reference Manual for the Calculation of Radionuclide Scrubbing in Water Pools (1991), Gesellschaft fuer Anlagen- und Reaktorsicherheit mbH (GRS), Koeln, Germany (as cited by Berna et al., 2016).

Rusche, H., Computational fluid dynamics of dispersed two-phase flows at high phase fractions (2003), Doctoral Thesis, Imperial College London (University of London), United Kingdom.

Turni, M., Experimental Study and Modeling of a Pool Scrubbing System for Aerosol Removal (2016), Tesi di Laurea, Politecnico di Milano, Italy.

Uchida, S., Itoh, A., Naitoh, M., Okada, H., Suzuki, H., Hanamoto, Y., Osakabe, M. and Fujikawa, M., Temperature dependent fission product removal efficiency due to pool scrubbing, Nuclear Engineering and Design, Vol. 298 (2016), pp. 201-207.

Wardle, K. and Weller, H., Hybrid multiphase CFD solver for coupled dispersed/segregated flows in liquid-liquid extraction, International Journal of Chemical Engineering (2013), pp. 1-13.

Wassel, A.T., Mills, A.F. and Bugby, D.C., Analysis of radionuclide retention in waterpools, Nuclear Engineering and Design, Vol. 90 (1985), pp. 87-104 (as cited by Berna et al., 2016).

[DOI: 10.1299/mej.23-00488]